A fully humanized von Willebrand disease type 1 mouse model as unique platform to investigate novel therapeutic options

Geneviève McCluskey,[1*] Marco Heestermans,[1*] Ivan Peyron,[1] Eloise Pascal,[2] Marie Clavel,[2] Eric Bun,[1] Emilie Bocquet,[1] Christelle Reperant,[1] Sophie Susen,[3] Olivier D. Christophe,[1] Cécile V. Denis,[1] Peter J. Lenting[1#] and Caterina Casari[1#]

[1]Université Paris-Saclay, INSERM, Hémostase Inflammation Thrombose HITh U1176, 94276, Le Kremlin-Bicêtre; [2]Inovarion, Paris and [3]Université de Lille, Inserm, CHU Lille, Institut Pasteur de Lille, U1011-EGID, F-59000 Lille, France

*GMC and MH contributed equally as first authors.
#PJL and CC contributed equally as senior authors.

Correspondence: C. Casari
caterina.casari@inserm.fr

Received: June 13, 2024.
Accepted: November 21, 2024.
Early view: November 28, 2024.

https://doi.org/10.3324/haematol.2024.286076

Abstract

Patients suffering from von Willebrand disease (VWD) have reduced quality-of-life despite current treatment options. Moreover, innovation in VWD therapeutic strategies has essentially stalled, and available treatments have remained unchanged for decades. Therefore, there is an unmet need to develop new therapeutic strategies for VWD patients, especially for the large portion of those with VWD-type 1. Due to species differences, the available VWD murine models are not suitable for preclinical studies, making it difficult to test new therapeutic approaches *in vivo*. With this in mind, we generated mice selectively expressing human von Willebrand factor (VWF) and human GPIbα. Because this fully humanized model was found to express low VWF (12%) and factor VIII (FVIII) (40%) levels with normal multimer profile and activity/antigen ratio, we repositioned it as a VWD-type 1 model (hVWD1 mice). In depth characterization of this model confirmed VWD-type 1 features with a decrease in platelet adhesion and thrombus formation *in vitro*. *In vivo*, a moderate bleeding phenotype was observed which was corrected upon the administration of recombinant-VWF or upon histamine-induced release of endothelial VWF. In search of new therapeutic options for VWD, we designed a bispecific single-domain antibody that bridges VWF to albumin (KB-V13A12). Remarkably, a single subcutaneous administration of KB-V13A12 coincided with a sustained 2-fold increase in VWF antigen levels for up to ten days and normalized hemostasis in a tail-clip model in hVWD1 mice. Here, we describe the development of our unique humanized mouse model for VWD-type 1 and a promising new therapeutic that corrected hemostasis in these mice.

Introduction

von Willebrand disease (VWD) is the most common inherited bleeding disorder, historically categorized into three main types and further subtypes.[1] In most reported cohorts, VWD-type 1 is the most frequent type (70-80% of cases). It consists of heterogeneous quantitative deficiencies with reduced von Willebrand factor (VWF) antigen levels between 5% and 30-50% (<30 regardless of bleeding, <50 with abnormal bleeding), usually normal activity-to-antigen ratios (>0.6), and normal or minimally abnormal multimer profiles.[1-3] Unsurprisingly, such a wide range of VWF levels is associated with variable phenotypes from minor to severe bleedings, which contribute to the challenge of diagnosing VWD-type 1/low VWF and precisely defining cut-off levels.[4,5] Genetics and pathogenesis of VWD-type 1 are again heterogeneous. VWF levels below 30% are often associated with bleedings and hereditary dominant genetic variants, whereas *VWF* DNA alterations are less common in low VWF patients with milder levels (30-50%).[6-10] Adding to the difficulties of VWD-type 1 diagnosis are fluctuating VWF levels, which may increase with age, during pregnancy, or after exercise. Finally, some of the bleeding symptoms typical of VWD-type 1 are also found in healthy individuals, although the severity may differ.[11,12] Due to this vast heterogeneity, the molecular mechanisms responsible for VWD-type 1 have not been fully elucidated. Diagnosis and management of patients with VWD-type 1 rely not only on laboratory results, but also on the personal and familial bleeding history, which remains challenging.[13] Desmopressin, an antidiuretic that promotes VWF release

from intracellular storage into the circulation, is the standard of care for these patients but has some disadvantages: 1) it remains ineffective in a small proportion of patients; 2) it is difficult to manage in children; 3) it is associated with tachyphylaxis; 4) it can induce minor side effects in some patients; and 5) it is only produced by one company, which causes supply issues.[14]

In the context of hemostasis, mouse models are irreplaceable tools to untangle the pathophysiology of disorders and to develop new therapeutic strategies. One of the major limitations of studying VWF in murine models is the human/mouse incompatibility between VWF and the platelet receptor GPIbα. In contrast to murine-(m)VWF, which can bind to human-(h)GPIbα *in vivo*, although with a reduced affinity,[15-17] human-VWF binds poorly to the murine receptor, preventing the normal recruitment of platelets at sites of injury. To overcome this limitation, several chimeric approaches have been developed.[17-19] The present study describes the first fully humanized murine model expressing full-length hVWF and hGPIbα. Because this model was found to recapitulate the characteristics of VWD-type 1, they will be referred to as hVWD1 mice throughout the manuscript. hVWD1 mice have a mild bleeding phenotype that can be rapidly but temporarily normalized by exogenous administration of recombinant hVWF concentrate or by the release of intracellular pools of VWF. Sustained hemostatic improvement was also observed with a bispecific single-domain antibody (sdAb) designed to increase VWF levels. Altogether, these engineered mice represent a new and exclusive platform for studying VWD-type 1 and appear to be a promising tool for developing and testing innovative therapeutic approaches for VWD.

Methods

A detailed description of the experimental procedures can be found in the *Online Supplementary Appendix*.

Animal and ethics statement

This project (n. APAFIS #32699-2021081611421076 v1) was approved by the local ethics committee of Université Paris-Saclay (Comité d'Ethique en Expérimentation Animale n. 26).

Engineering of hVWD1 mice

Transgenic mice expressing hVWF and hGPIbα instead of the corresponding murine proteins (Figure 1A, B) were engineered in a pure 129S2 genetic background known to express functional ADAMTS13 (a disintegrin and metalloproteinase with a thrombospondin type 1 motif, member 13)[20,21] (genOway, Lyon, France). 129S2Crl-*Vwf*$^{-/-}$-Tg(*VWF*) mice and 129S2Crl-*Gp1ba*$^{-/-}$-Tg(*GP1BA*) mice, were intercrossed to generate double knock-in mice 129S2Crl-*Vwf*$^{-/-}$-Tg(*VWF*),*Gp1ba*$^{-/-}$-Tg(*GP1BA*), which will henceforth be referred to as hVWD1. Littermate controls will be referred to as 129S2 (Figure 1C).

Polymerase chain reaction (PCR) products for genotyping were separated by electrophoresis (Figure 1D).

von Willebrand factor-factor VIII assays

von Willebrand Factor antigen (VWF:Ag) levels[22] and multimer profiles[23,24] were assessed as previously described. VWF activity was measured with a collagen binding (VWF:CB) and a platelet-dependent (VWF:GPIbR) assay. FVIII activity (FVIII:C) was measured using the chromogenic Biophen FVIII-assay kit (Hyphen, Neuville-sur-Oise, France) according to the manufacturer's instructions.

Parallel plate flow perfusion

Thrombus formation was evaluated using a Maastricht flow chamber in a whole-blood perfusion assay on a fibrillar collagen matrix under arterial shear conditions (shear rate of 3000 s^{-1}). Single dots in the graph represent individual mice (average value of 20 images).

KB-V13A12 production and administration

Single-domain antibodies against VWF were generated;[25] sdAb KB-V13 (formerly KB-VWF-013) binding h/mVWF has been previously characterized.[26] KB-V13 recognizes the D'D3 region of VWF and does not interfere with the FVIII binding to VWF. The anti-albumin KB-OptiAlb12 is a llama-derived sdAb that displays high-affinity binding (<5 nM) to both human and murine albumin. KB-V13A12, combining the two sdAb, was expressed in competent *E. coli* WK6 bacteria and purified by affinity chromatography. A control bispecific sdAb (KB-V13AT02) was synthetized by cloning the KB-V13 linked to the previously described KB-AT02 against antithrombin.[27]

Purified bispecific sdAb were administered subcutaneously (SC) (5 mg/kg body weight).

Tail vein transection model and tail artery transection model

Tail vein transection (TVT) was conducted as previously described.[28] The tail artery transection (TAT) model consisted of a modified TVT in which the ventral tail artery was transected using the same customized templates. The post-incision observation time was set at 30 minutes (min).

Tail-clip model

A tail-clip assay was performed as previously described.[29,30] Histamine (Merck, Fontenay Sous Bois, France) was administered intraperitoneally (13 µmol/kg body weight)[31] 30 min prior to the procedures.

Recombinant hVWF (r-hVWF, Veyvondi, Takeda) was administered intravenously (IV) (50 U/kg body weight) 5 min before the procedures.

Saphenous vein puncture model

The saphenous vein puncture model was conducted as previously described.[32]

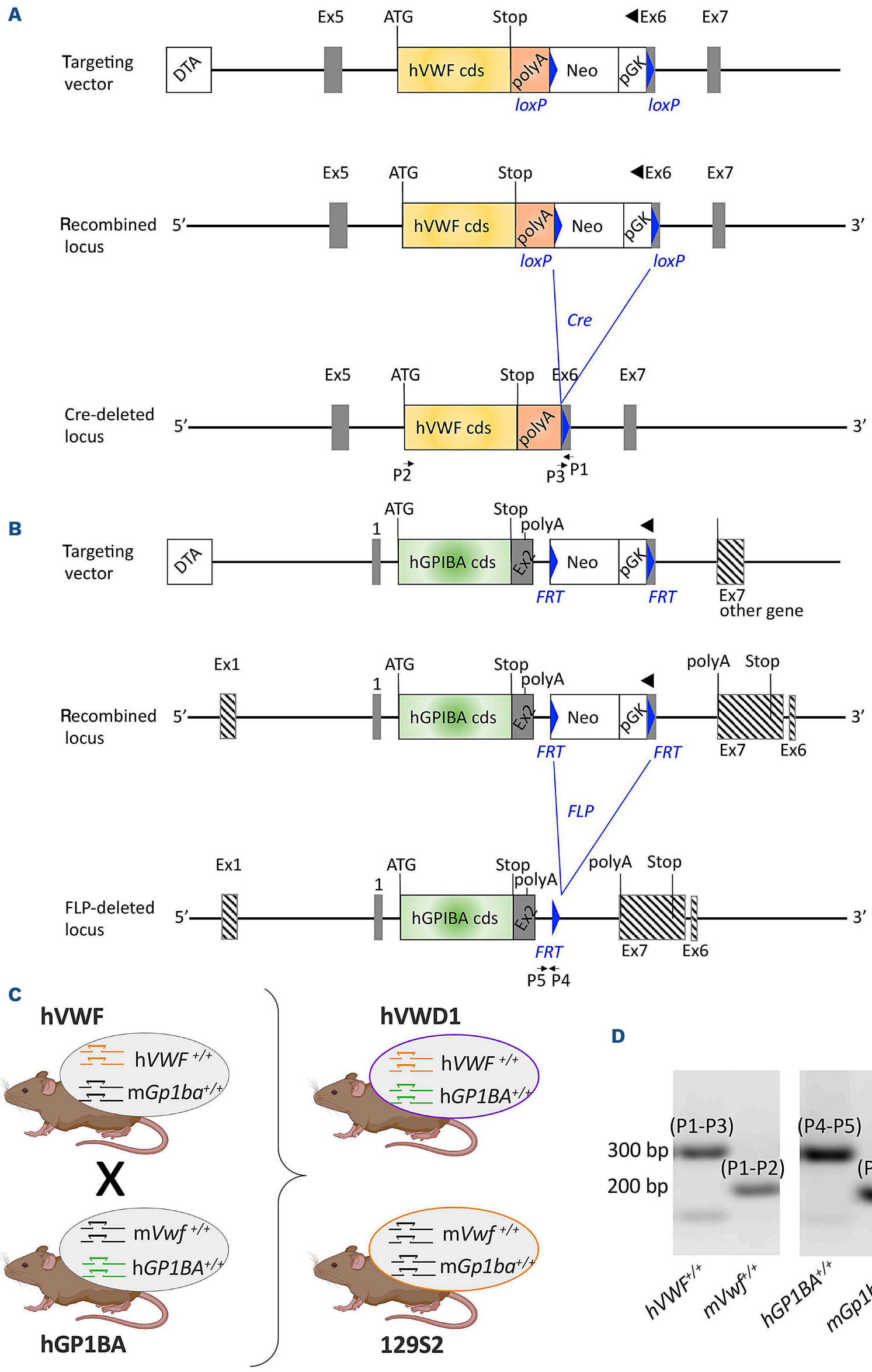

Continued on following page.

Figure 1. Engineering of hVWD1 mice. (A) Targeting vector comprising the whole coding sequence (cds) of *human VWF* followed by a hGH (human growth hormone) polyadenylation site (polyA). A neomycin positive selection cassette (Neo) flanked by two loxP sites was inserted downstream of the polyA site and a Diphteria toxin negative selection cassette (DTA) was inserted outside the homologous recombination area, upstream of exon 5. Following homologous recombination and double selection of embryonic stem cells (ES), the recombined locus bore the *hVWF* cds followed by a Neo cassette flanked by two loxP sites. After injection of ES cells into blastocysts and breeding of the generated mice with 129Sv Cre-deleter mice, the Neo cassette was excised and heterozygous mice carrying the mutant allele were generated. Heterozygous mice were intercrossed to generate homozygous 129S2Crl-*Vwf*$^{-/-}$-Tg(*VWF*) mice, named hVWF. (B) Targeting vector comprising the whole cds of *human GP1BA*. A Neo positive selection cassette flanked by two FRT sites was inserted downstream of the polyA site and a DTA negative selection cassette was inserted outside the homologous recombination area, upstream of exon 1. Following homologous recombination and double selection of embryonic stem cells, the recombined locus bore the *hGP1BA* cds followed by a Neo cassette flanked by two FRT sites. After injection of ES cells into blastocysts and breeding of the generated mice with 129Sv FLP-deleter mice, the Neo cassette was excised and heterozygous mice carrying the mutant allele were generated. Heterozygous mice were intercrossed to generate homozygous 129S2Crl-*Gp1ba*$^{-/-}$-Tg(*GP1BA*) mice, named hGP1BA. (C) Schematic of the breeding strategy. Homozygous hVWF and hGP1BA were crossed to generate double-transgenic mice, referred to as hVWD1, and control mice, referred to as 129S2 mice. (D) Representative PCR products in transgenic mice expressing human or murine *VWF* and *GPIba*. Primers P1, P2, P3, P4, and P5 as indicated in (A) and (B). Primer sequences are reported in *Online Supplementary Table S1*.

Thrombosis model

In vivo thrombus formation in the carotid artery was induced by 15% ferric-chloride.

Statistical analysis

All data are presented as mean±standard deviation (mean±SD). Numbers (N) refer to individual animals. The statistical analysis was performed using GraphPad Prism 10 software (La Jolla, CA, USA). One-way analysis of variance (one-way ANOVA) followed by Tukey or Dunnett multiple comparison test was performed when comparing multiple groups. Pairwise analysis was performed using the unpaired two-tailed Student *t* test, unless otherwise stated. Two-way analysis was performed for two factor comparisons. $P<0.05$ was considered statistically significant.

Results

hVWD1 mice are viable and fertile

hVWD1 mice expressing hVWF (wild-type) and hGPIbα (wild-type) were generated using the targeting strategy outlined in Figure 1. Intercross of heterozygous mice for each transgene to obtain homozygous mice 129S2Crl-*Vwf*$^{-/-}$-Tg(*VWF*) named hVWF mice and 129S2Crl-*Gp1ba*$^{-/-}$-Tg(*GP1BA*) named hGP1BA mice, resulted in mendelian distribution of genotypes (*data not shown*), suggesting that expression of the human version of VWF and GPIbα proteins in mice does not impair murine embryonic development or perinatal survival. Homozygous hVWF and hGP1BA mice were then intercrossed to obtain homozygous, double humanized mice, named hVWD1 (129S2Crl-*Vwf*$^{-/-}$-Tg(VWF), *Gp1ba*$^{-/-}$-Tg(GP1BA)) (Figure 1C).

hVWD1 mice express human von Willebrand factor and have a normal multimer profile

Because hVWD1 mice express hVWF and littermate controls express mVWF, VWF:Ag levels cannot be compared in the two groups of mice. Therefore, VWF:Ag levels for hVWD1 mice were quantified using human pooled normal plasma (hPNP) as reference; average VWF:Ag levels were 12±3% (N=51) (Figure 2A). VWF activity was measured with a VWF:CB and a VWF:GPIbR assay. Activity/antigen ratios were similar for the two assays (0.8±0.2, N=7) (Figure 2B). FVIII:C levels were also reduced compared to control mice (40±9% and 117±17%, respectively; $P<0.001$) (Figure 2C). Both VWF:Ag and FVIII:C levels were relatively stable over a 15-17-week time period (*Online Supplementary Figure S1A, B*).

Despite the quantitative defect, multimer profiles of plasmatic VWF showed normal distribution of low, medium, and high molecular weight multimers (HMWM), consistent with VWD-type 1 profiles in patients (Figure 2D, lanes 1-2). Multimers were characterized by the typical triplets that are also observed in human plasma, suggesting that hVWF expressed in mice is cleaved by mADAMTS13 in a similar way as in humans (Figure 2D, lanes 3-4).

The presence of hVWF was validated in an immunosorbent assay using monoclonal antibodies selectively recognizing hVWF (*Online Supplementary Figure S2*). Although in an indirect manner, these analyses also supported the absence of mVWF in hVWD1 mice. Exclusive human or murine GPIbα expression on platelets was validated by flow cytometry using species-specific monoclonal antibodies (*Online Supplementary Figure S3*) and by immunofluorescence on blood smears (*data not shown*).

Mice expressing hGPIbα have been generated previously with a similar genetic approach and their platelets and GPIb-IX-V complex characterized.[15,16] We tested platelet counts, volume, and activation (*Online Supplementary Figure S4*). Peripheral platelet count was modestly decreased in hVWD1 compared to control mice (471±47 and 592±65x10^9/L, respectively; $P<0.001$) (*Online Supplementary Figure S4A*), while platelet size was moderately increased (6±0.3 and 5±0.3 fl, (*Online Supplementary Figure S4B*). Despite these minor differences, agonist-induced platelet activation was similar between the two groups (*Online Supplementary Figure S4C, D*).

We also assessed VWF in platelets and found that hVWD1

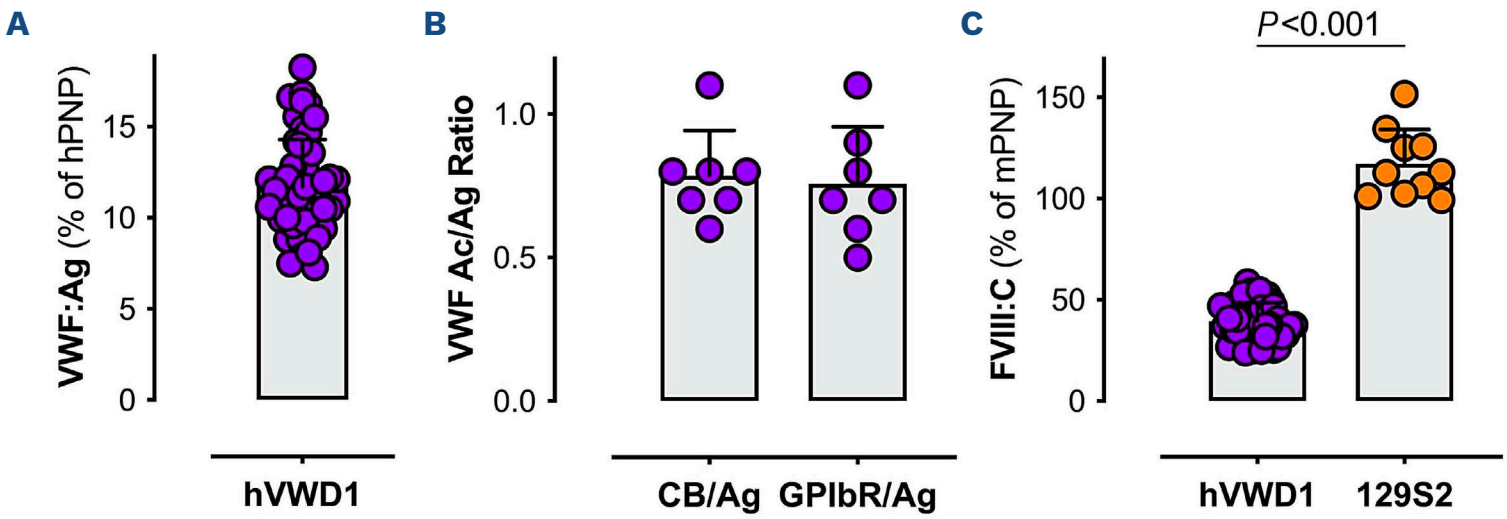

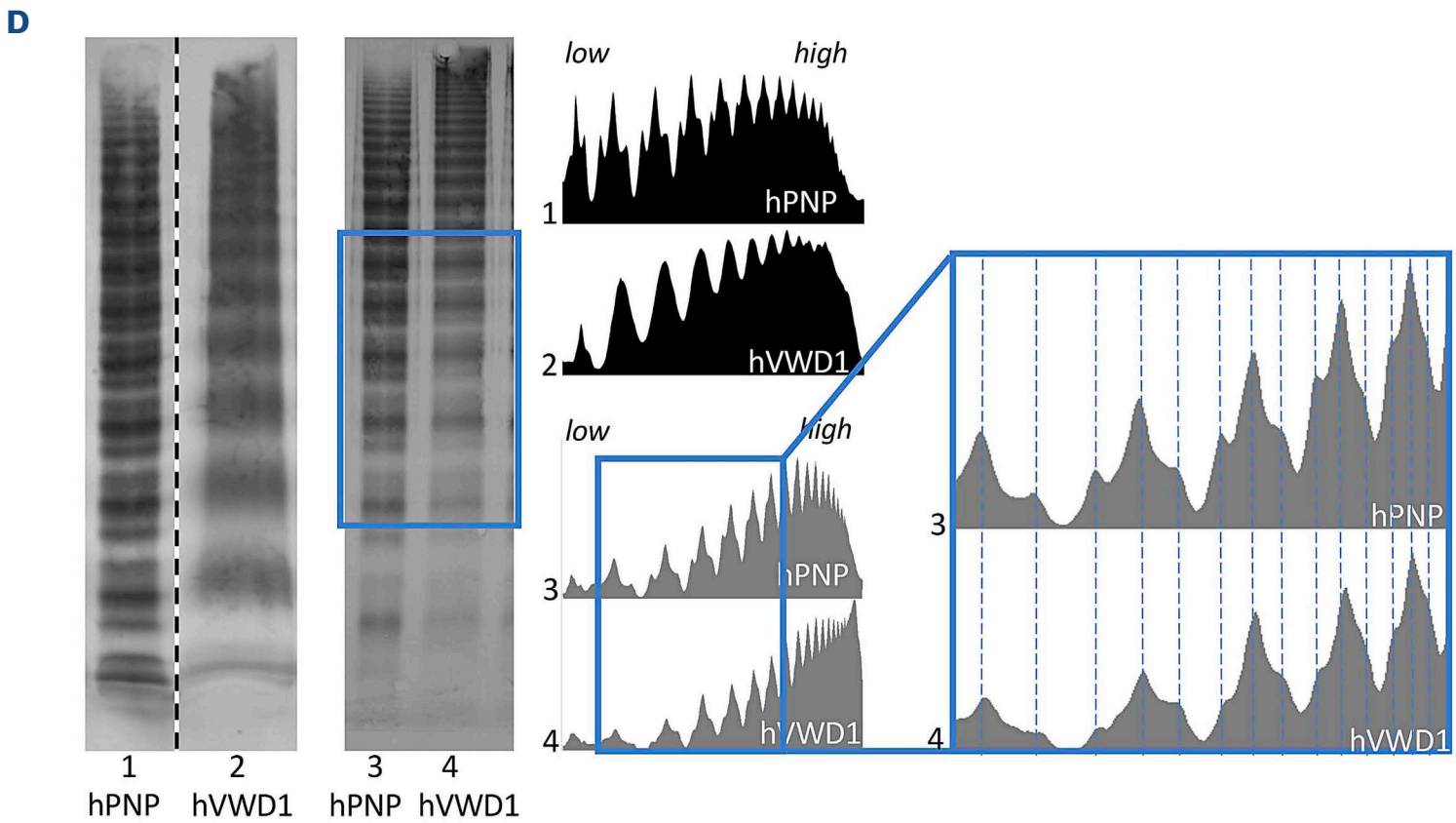

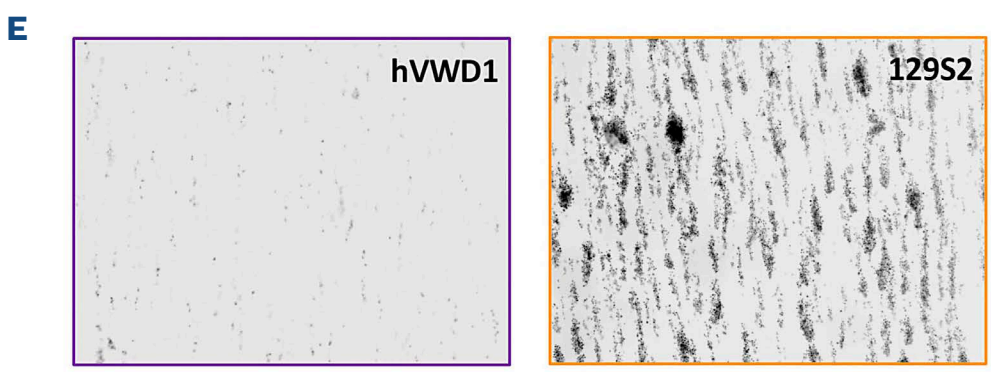

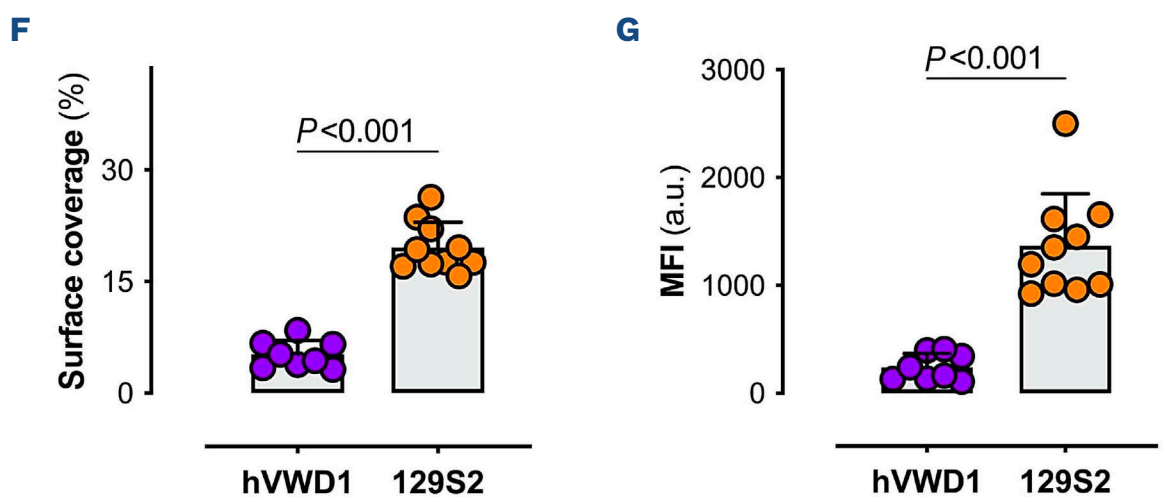

Continued on following page.

Figure 2. von Willebrand factor and factor VIII in hVWD1 mice. (A) von Willebrand factor (VWF) antigen (VWF:Ag) levels in von Willebrand disease-type 1 (hVWD1) mice compared to a human pooled normal plasma (N=51). (B) VWF activity/antigen ratio for hVWD1 mice (N=7). VWF activity was assessed in a VWF:CB and a VWF:GPIbR assays. (Normal ratios >0.7). (C) Factor VIII activity (FVIII:C) levels in hVWD1 mice (N=42, purple) and control mice (N=10, yellow) compared to murine pooled normal plasma. (D, left) Representative plasmatic VWF multimer profiles in 2% agarose gels. Colorimetric detection. Lanes 1 and 2 were prepared with standard sample dilution and similar amount of total VWF loaded (approx. 25 ng). Lanes 3 and 4 were prepared to minimize the amount of murine plasma loaded in each sample. Total amount of VWF was approximately 15 ng. The dotted line indicates non-adjacent lanes on the same gel. Lanes 3 and 4 were loaded on a different gel. (D, center) Densitometric analysis of multimers in (D). (D, right) Triplet structures are shown at higher magnification for some of the profiles (blue boxes). (E) Representative images of thrombi formed during perfusion of blood collected from hVWD1 (left) and control (right) mice over a collagen-coated surface at 3000 s^{-1}. Pictures were randomly selected over a total of 160-200 acquired images (20 images/perfusion; every perfusion was performed with blood collected from individual mice). (F and G) Quantification of the percentage of surface covered by platelets (F) and mean fluorescence intensity (MFI) (G) in hVWD1 mice (N=8, purple) *versus* control mice (N=10, yellow). (A, B, C, F, G) Gray bars indicate mean±standard deviation. (C, F, G) Unpaired two-tailed Student *t* test. a.u.: arbitrary units; low: VWF-low molecular weight multimers (MWM); high: high MWM.

mice have a minor reduction in platelet-VWF content, compared to human platelets or 129S2-platelets (*Online Supplementary Figure S5*). Importantly, platelet-VWF was slightly enriched in HMWM, similar to VWF in human platelets (*Online Supplementary Figure S5*).

von Willebrand factor function was evaluated using classic parallel plate perfusion chambers at elevated shear rate (3000 s^{-1}), at which platelet tethering is highly dependent on VWF.[33,34] Consistent with low VWF:Ag in circulation and minor platelet-VWF reduction, only some small thrombi were formed in hVWD1 mice (Figure 2E). Platelet-covered surface and fluorescence intensity were 4-6-fold decreased compared to control mice (% of covered-surface 5.2±1.9 *vs*. 19.6±3.4, fluorescence a.u. 241±126.2 *vs*. 1,367±480.2, respectively; *P*<0.001) (Figure 2F, G), suggesting that the reduced VWF levels are insufficient to support normal thrombus formation in hVWD1 mice.

hVWD1 have a mild bleeding phenotype and a modestly reduced response to ferric chloride

To thoroughly characterize this model of VWD-type 1, hemostasis and thrombosis were assessed using *in vivo* assays of various severity. First, the difference between the amount of blood shed by hVWD1 and control mice was not statistically significant (84±82 and 36±22 μl, respectively; *P*=0.1223) (Figure 3A) when assessed in the TVT model. In addition, bleeding profiles were similar between both groups (Figure 3B), showing that hVWD1 mice exhibited similar hemostasis as control mice in this particular model. We next applied more severe models. In a TAT assay, the bleeding tendency of hVWD1 mice was higher than that of control mice, with 2-fold more blood shed from the injury (511±232 and 245±184 μl, respectively; *P*=0.0082) (Figure 3C) and longer bleeding times in hVWD1 mice (Figure 3D). In a tail-clip assay, despite some variability, the amount of blood shed over 30 min was increased 5-fold in hVWD1 mice compared to control mice (102±122 and 18±37 μl, respectively; *P*=0.0004) (Figure 3E) and the time of the first bleeding arrest was substantially delayed (463±624 seconds in hVWD1 mice and 88±49 seconds in control mice; *P*=0.0095) (Figure 3F). Finally, in a model of large saphenous vein puncture, the number of clots formed during the 30-min observation time, was notably decreased in hVWD1 *versus* control mice (12±5 *vs*. 20±4 clots, respectively; *P*<0.0001) (Figure 3G), which also coincided with relatively longer bleeding times (*data not shown*). Overall, these data indicate that hVWD1 mice display a moderate bleeding phenotype recapitulating the profile of a large proportion of patients with this disease.

In addition, we evaluated $FeCl_3$-induced thrombus formation in the carotid artery of hVWD1 mice and control mice. hVWD1 had reduced response to $FeCl_3$ (Figure 4). The decrease in blood flow upon $FeCl_3$ administration, a proxy for progressive vessel occlusion, was slower and less pronounced in hVWD1 mice than in control mice, resulting in a higher area under the curve (697±267 *vs*. 393±121 a.u., respectively; *P*=0.0260) (Figure 4A, B). Occlusion was delayed in hVWD1 mice but failed to reach a statistically significant difference between both groups (14±8.1 *vs*. 8.1±2.2 seconds, respectively; *P*=0.0649; one out of 6 hVWD1 did not occlude) (Figure 4C).

Recombinant human von Willebrand factor is functional and restores hemostasis in hVWD1 mice

We evaluated whether restoring VWF normal levels using r-hVWF would be functional in our hVWD1 mice. Mice were administered 50 U/kg of r-hVWF (therapeutic dose) and VWF antigen, multimers, and hemostasis were assessed 5 min post IV injection. VWF:Ag levels increased approximately 6-fold post infusion, reaching 76±5.2% (Figure 5A). As expected, when evaluated in medium-resolution gels, multimer profiles were similar before and post r-hVWF administration; however, due to higher protein concentration, bands corresponding to multimers of almost all molecular weight appeared sharper post infusion (Figure 5B, C). Densitometry suggested that r-hVWF administration resulted in an enrichment of medium-MWM (Figure 5C). A separate group of mice were subjected to a tail-clip assay (Figure 5D). The amount of blood shed by hVWD1 mice receiving r-hVWF (64±82 μl, magenta) was similar to that shed by control mice (19±37 μl, yellow) (*P*=0.5290) and coincided with normalization of the bleeding time (*data not shown*).

A *Tail-vein-transection assay*

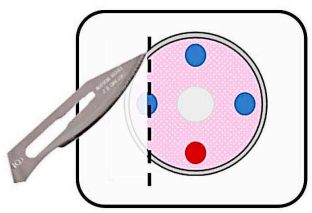

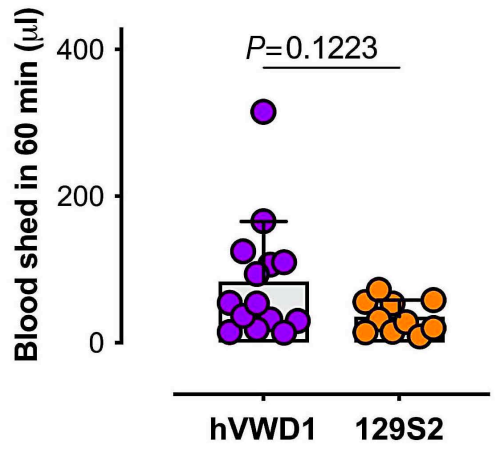

B

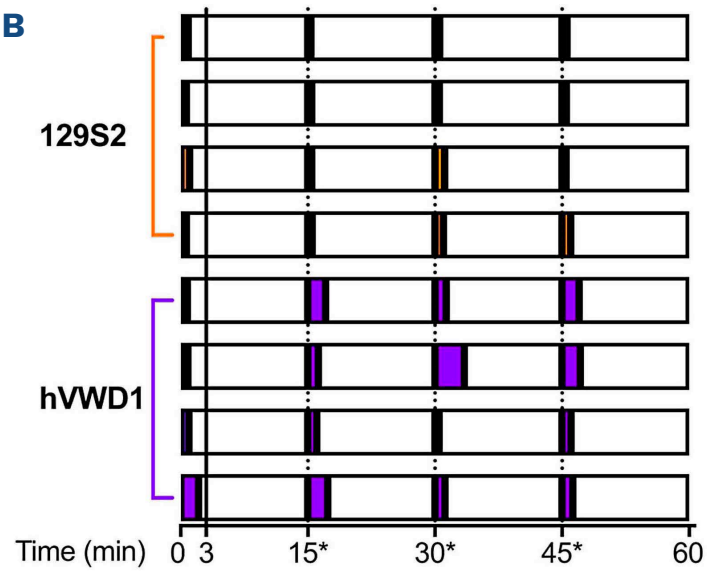

C *Tail-artery-transection assay*

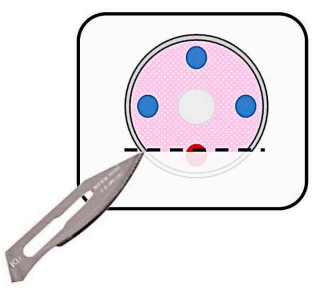

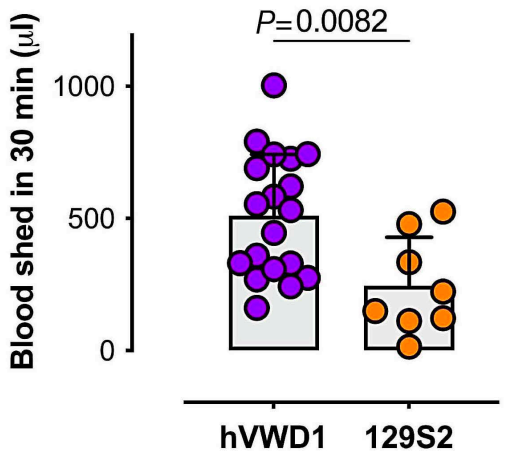

D

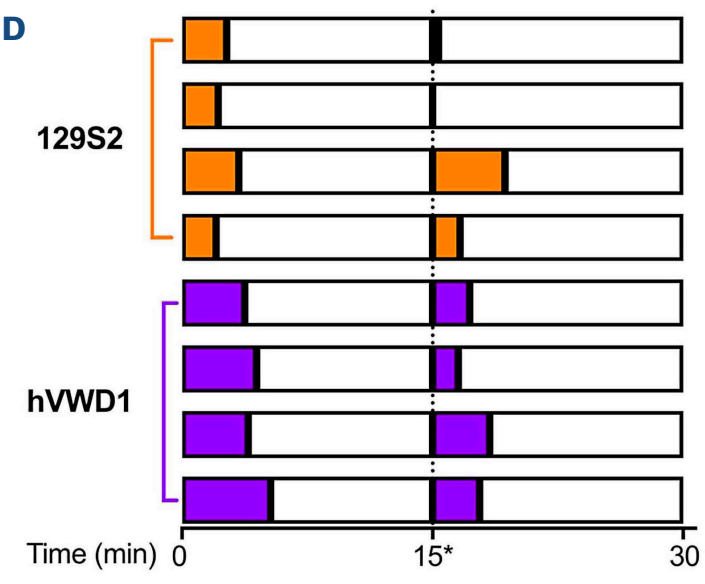

E *Tail-clip assay*

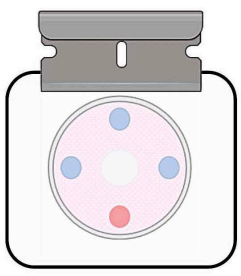

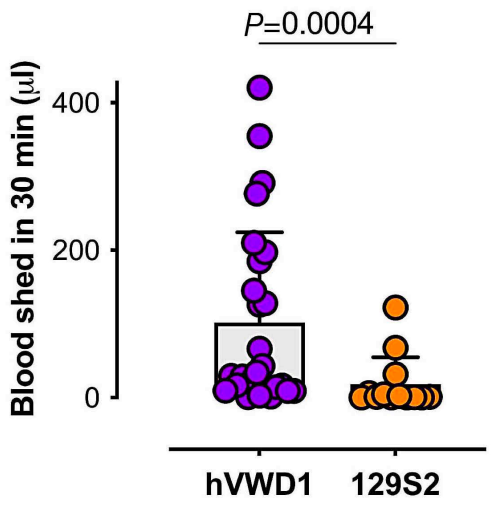

F

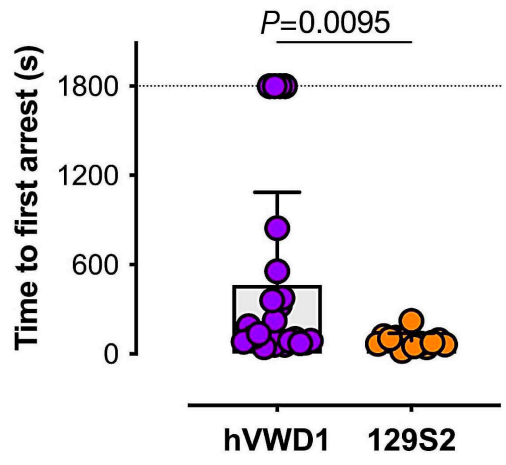

G *Saphenous vein puncture assay*

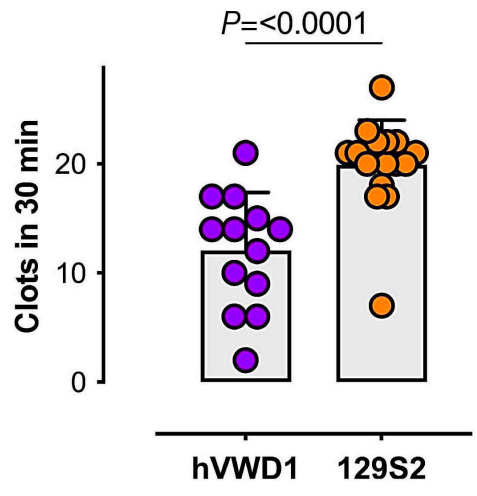

Continued on following page.

Figure 3. Hemostasis is mildly altered in hVWD1 mice. (A) Schematic representation of a tail-vein-transection (TVT) assay indicating the injured vessel. Amount of blood shed by von Willebrand disease-type 1 (hVWD1) mice (N=14, purple) and control (N=10, yellow) mice during the 60-minute (min) experimental time. (B) Representative bleeding profiles in the two groups of mice. Filled bars indicate active bleedings, empty bars indicate non-bleeding periods. Dotted lines at 15-30 and 45 min indicate clot removal (challenge). (C) Schematic representation of a tail-artery-transection assay (TAT). Amount of blood shed by hVWD1 (N=19) and control mice (N=8) during 30 min. (D) Representative bleeding profiles. Filled and empty bars as in (B). (E) Schematic representation of a tail-clip assay and of the severed vessels. Amount of blood shed by hVWD1 (N=26) and control (N=13) mice during the 30-min long experiment. (F) Time of first bleeding arrest upon the injury in the two groups of mice. (G) Schematic representation of a saphenous vein puncture assay. The number of clots formed upon the first incision in hVWD1 (N=13) and control (N=17) mice in 30 min. (A, C, E-G) Gray bars indicate mean±standard deviation. (A, E-G) Mann-Whitney test. (C) Unpaired two-tailed Student *t* test.

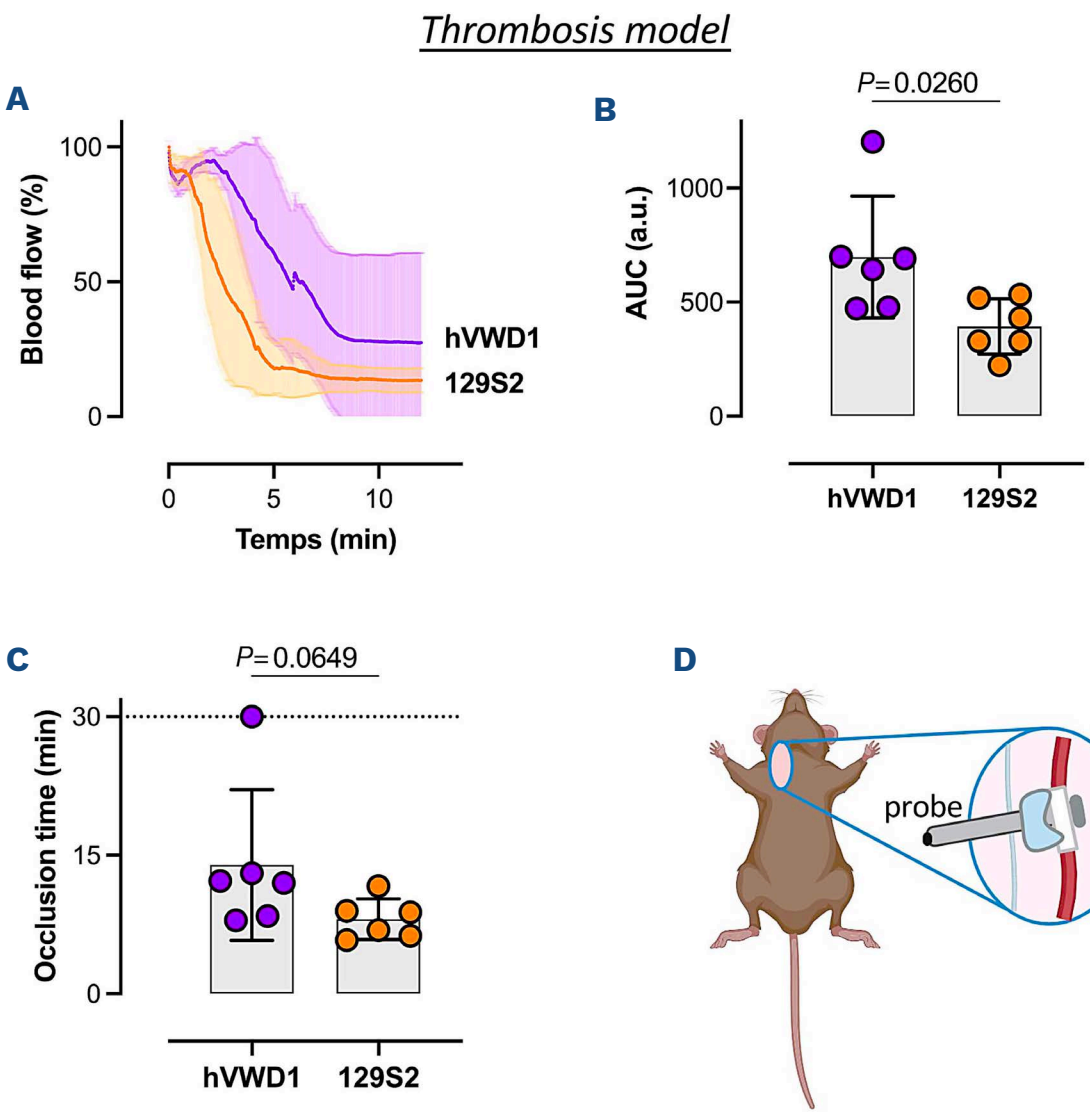

Figure 4. Ferric chloride-induced thrombus formation. (A) Carotid artery blood flow measured post-$FeCl_3$-induced endothelial damage in von Willebrand disease-type 1 (hVWD1) mice (purple) and control (yellow) mice. Initial blood flow was similar in all mice and set at 100% for normalization purposes. The graph indicates average curves (colored lines) and standard deviation (SD) (filled area); N=6 per group of mice. (B) Statistical analysis was performed by comparing the area under the curve (AUC) of individual curves for hVWD1 and control mice. (C) Occlusion times were measured. An occlusive event was indicated by flow <0.2 mL/minute (min) for a minimum of 10 min. (D) Schematic representation of the *in vivo* thrombus-formation model. Ferric chloride was administered by gentle deposition of a wet filter paper on the exposed vessel (white rectangle) for 2 min. The paper was then removed and the probe placed at the same position for flow monitoring. (B and C) Gray bars indicate mean±standard deviation; Mann-Whitney test. AUC: area under the curve; a.u.: arbitrary unit.

These data demonstrate that r-hVWF is functional and restores hemostasis in hVWD1 mice.

Agonist-induced release of endothelial human von Willebrand factor restores hemostasis in hVWD1 mice

To explore whether intracellular VWF could be released in circulation and affect hemostasis, we triggered histamine-induced endothelial degranulation (as a surrogate for desmopressin).[31] Thirty minutes after intraperitoneal administration of histamine to hVWD1 mice, circulating VWF:Ag was significantly increased in 14 out of 15 mice (from 13±3% to 17±2%; *P*<0.0001) (Figure 6A). Because VWF stored in Weibel-Palade bodies is known to be enriched in HMWM, we also performed multimer analysis. To minimize inter-gel differences, plasmas collected from the same mouse before and after histamine administration were loaded in consecutive lanes after normalization of VWF concentrations (Figure 6B). Densitometric analysis showed that multimer profiles were shifted toward increased levels of HMWM post- (black profiles) compared to pre-injection (gray) (Figure 6C) in the majority of mice (8 out of 11). Despite the variable antigen response, the quantitative increase, paired with the multimer improvement, was sufficient to sustain hemostasis in the tail-clip model (19±37 µl control mice [yellow] and 48±62 µl hVWD1 mice [blue] receiving histamine; *P*=0.6928) (Figure 6D). These data indicate that, similar to humans, hVWD1 mice have a pool of highly multimerized, functional VWF, which can be rapidly released in circulation.

hVWD1 mice are instrumental in developing new therapeutic molecules: the example of KB-V13A12

Despite currently available treatments for patients with VWD-type 1 being considered quite effective, recurrent

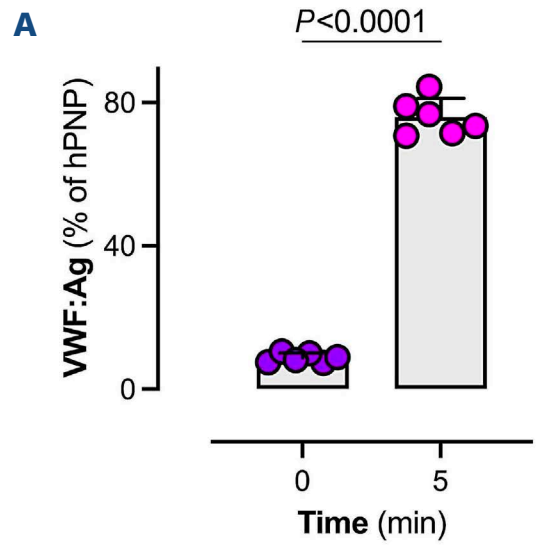

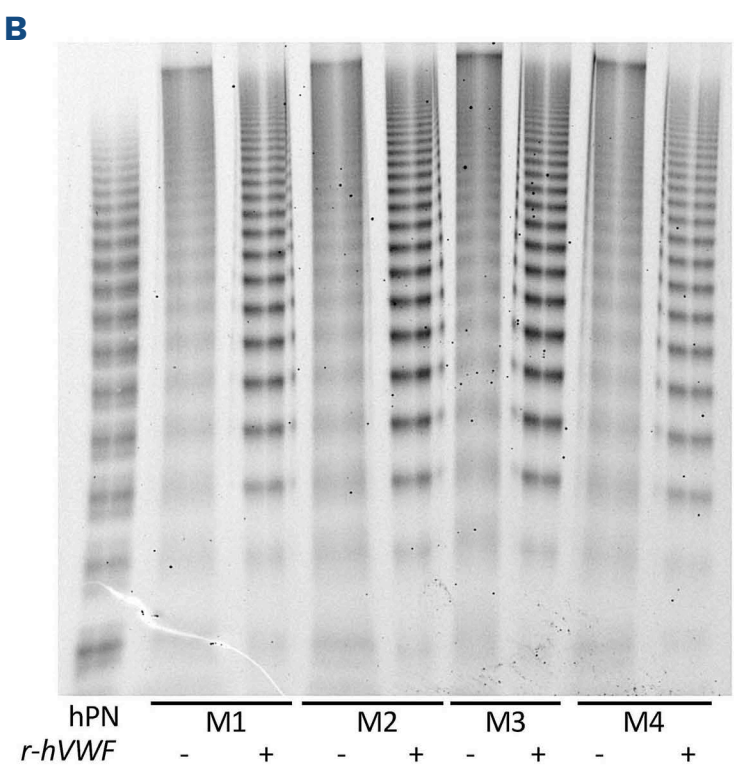

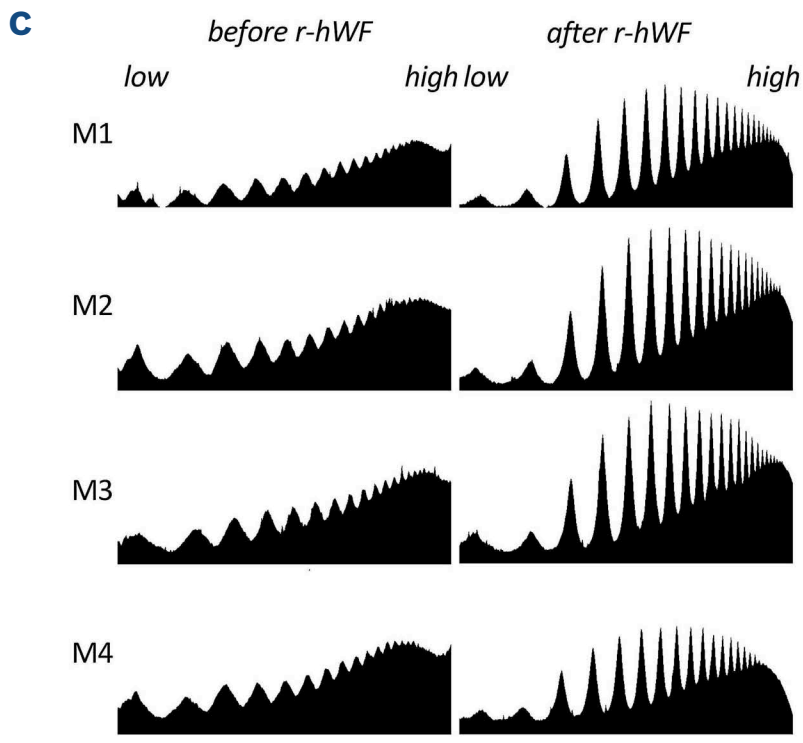

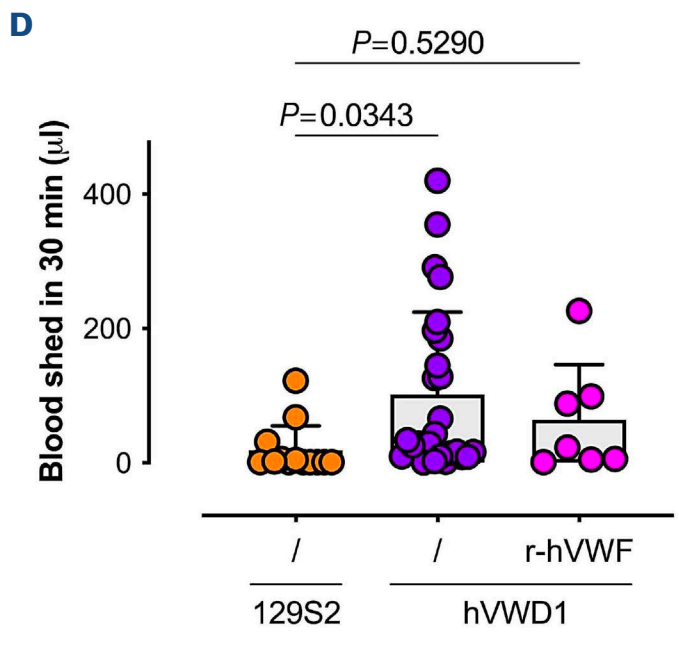

Figure 5. Recombinant human von Willebrand factor administration restores hemostasis in hVWD1 mice. (A) von Willebrand factor (VWF) antigen levels in von Willebrand disease-type 1 (hVWD1) mice before (purple) and 5 minutes (min) post (magenta) r-hVWF administration (N=6). (B) Representative multimer profiles in 1.5% agarose gel. Fluorescent detection. Similar total amount of VWF loaded in consecutive lanes corresponding to samples collected from the same mouse (6-10 ng). (C) Densitometric analysis of multimers in (B). Profiles on the left are before and profiles on the right are post r-hVWF infusion. (D) Amount of blood shed in 30 min by control mice (N=13, yellow), untreated hVWD1 mice (N=26, purple), and treated hVWD1 mice (N=7, magenta). (A-D) Gray bars indicate mean±standard deviation. (A) Paired two-tailed Student *t* test. (D) One-way ANOVA with Dunnett correction for multiple comparisons. low: VWF-low molecular weight multimers (MWM); high: high MWM.

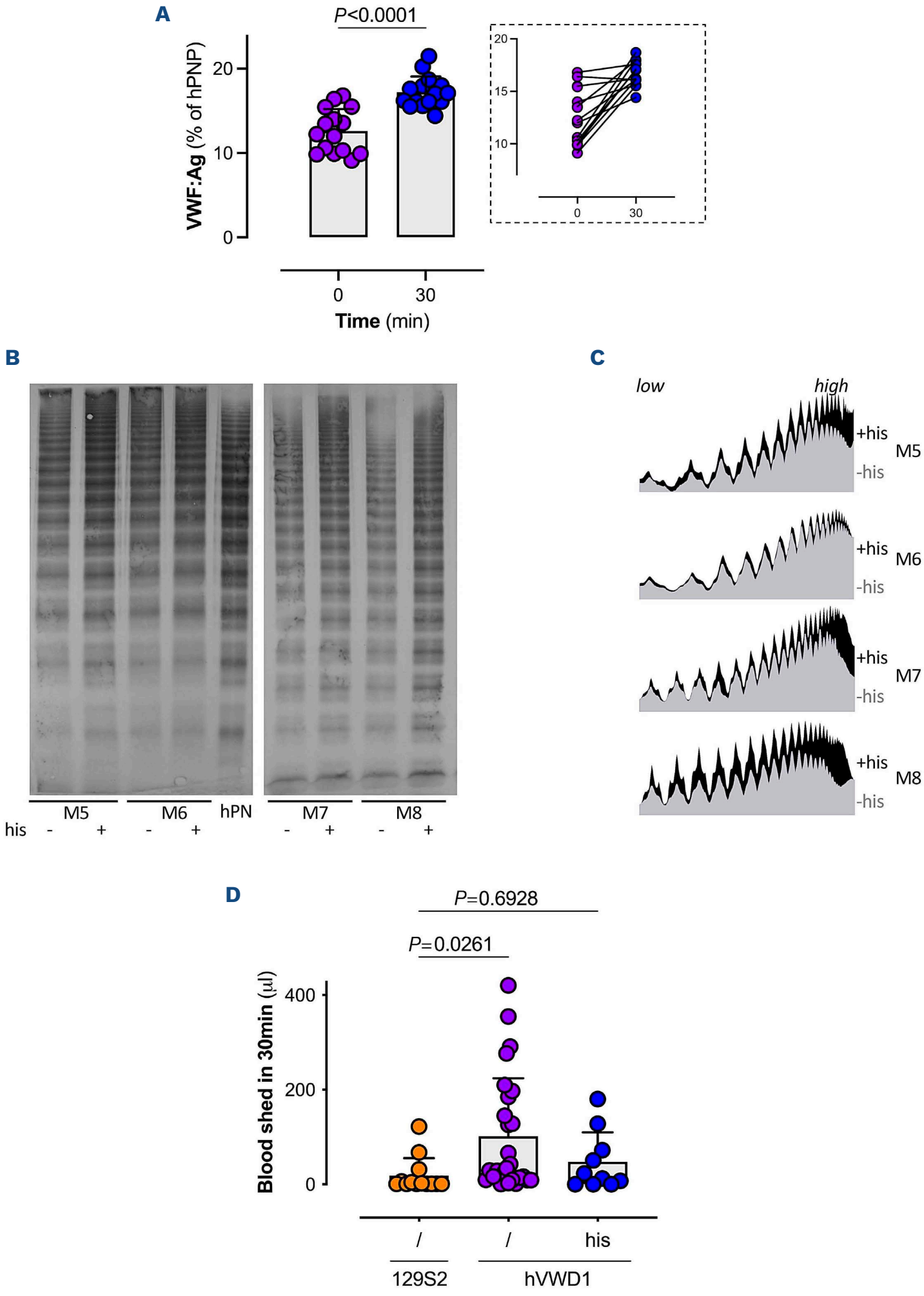

Figure 6. Histamine-induced endothelial degranulation rapidly restores hemostasis in hVWD1 mice. (A) von Willebrand factor (VWF) antigen levels in human von Willebrand disease-type 1 (hVWD1) mice before (purple) and 30 minutes (min) post (blue) histamine administration (N=15). Levels of individual mice are indicated in the inset. (B) Representative multimer profiles in 2% (left) or 1.5% (right) agarose gels. Colorimetric detection. Similar total amount of VWF (15-20 ng) loaded in each consecutive lane. White space separates two distinct gels. (C) Densitometric analysis of multimers in (B). Profiles of samples collected from the same mouse, before (gray) and post (black) histamine infusion are superposed. (D) Amount of blood shed in 30 min by control mice (N=13, yellow), untreated hVWD1 mice (N=26, purple), and treated hVWD1 mice (N=10, blue). (A-D) Gray bars indicate mean± standard deviation. (A) Paired two-tailed Student *t* test. (D) One-way ANOVA with Dunnett correction for multiple comparisons. low: VWF-low molecular weight multimers (MWM); high: high MWM.

bleedings are still reported, especially in patients with the potential to menstruate suffering from menorrhagia.

In search of novel therapeutic options, we generated a bispecific antibody composed of a non-inhibitory anti-VWF(D'D3) sdAb[26] linked to an sdAb recognizing human and murine albumin, named KB-V13A12.[35] While thorough characterization of this bispecific sdAb will be discussed in a separate study (Peyron *et al.*, unpublished data), the hVWD1 mice seemed to be the perfect platform to test this molecule. Following its administration (5 mg/kg), VWF levels were determined over a 14-day period, while the tail-clip procedure was performed three days after administration in another series of mice. The 5 mg/kg dose was selected based on a dose-effect curve (*Online Supplementary Figure S6*). Remarkably, VWF antigen levels rapidly increased one day post injection, achieving a relatively stable near 2-fold increase between 3- and 10-day post-injection (11±2% pre- *vs*. 21±3% 3-day post- and 19±3% 10-day post-administration; $P<0.0001$) (Figure 7A, [green]). As a control, the administration of a bispecific sdAb targeting VWF and antithrombin (KB-V13AT02) had no effects on VWF levels (Figure 7A, [gray]).

We also tested two conditions for multimer analysis. First, the total amount of VWF was normalized (Figure 7B, samples M9-M10) at the expense of having to use different ratios of plasma and buffer between pre- and post-administration samples. In these conditions, we observed that the overall multimer profile remained unaffected by administration of KB-V13A12 (Figure 7C). Triplets were visible only in post-administration samples having the lower plasma/buffer ratio. Consistent with normal triplet structure, the central band was more intense compared to satellite bands, suggesting that VWF degradation was not perturbed. In the second condition, we loaded the maximum amount of VWF for each sample, keeping the plasma/buffer ratio identical between pre- and post-treatment samples (Figure 7B, C, samples M11-M12). In these conditions, multimers of all molecular weight appeared increased post KB-V13A12 infusion, suggesting that the sdAb is able to bind multimers of any molecular size.

Finally, tail-clip was performed three days post treatment (Figure 7D). One single SC administration of KB-V13A12 was sufficient to restore hemostasis of hVWD1 mice by normalizing the amount of blood shed upon injury in a quite severe bleeding model (19±37 µl in control mice) (Figure 7D, [yellow]) and 47±49 µl in hVWD1 mice (Figure 7D, [green]) receiving KB-V13A12 ($P=0.7111$).

Discussion

Von Willebrand disease-type 1 is the most frequent VWD-type but also one of the most heterogeneous, making it difficult to diagnose and manage, especially in patients with mild VWF levels, also referred to as low VWF.[4,12] Despite the high prevalence of this VWD-type, the only murine model available so far has been the RIIIS/J mouse expressing low levels of mVWF, FVIII, and Factor XI.[36,37] These mice have been instrumental in linking aberrant post-translational modifications to elevated VWF clearance; however, their use as models to test therapeutic molecules is limited. In the present study, we report on the fortuitous creation and characterization of the first fully humanized VWD-type 1 model (hVWD1 mice) and its unique use as a platform to test new therapeutic strategies, one of which is presented here.

Patients with VWD-type 1 and VWF levels below 30% often carry dominant genetic variants within the *VWF* gene. The hVWD1 mice express low levels (approx. 12%) of normal hVWF without any pathological genetic variant within the *VWF* gene. Several mechanisms associated with genomic engineering could contribute to these low levels and are not mutually exclusive: a) the absence of intronic regulatory sequences, missing because only the h-cDNA has been inserted in the m-genome; b) expression of the hVWF under the control of endogenous murine regulatory elements, which have not been humanized; and c) structural differences due to genomic rearrangements somehow affecting transcription of the h-cDNA and protein expression.

One major functional complication needs to be carefully considered when expressing hVWF in murine models. VWF accomplishes its functions by binding to its partners and, during primary hemostasis, it is essential to initiate tethering of platelets to the sub-endothelium at sites of vascular injury. However, due to a human/mouse incompatibility between VWF and GPIbα, hVWF interacts poorly with murine platelets. In the past, to overcome this limitation, our group and others have engineered one partner or the other by creating chimeric models able to sustain VWF/platelet interaction.[17-19] To the best of our knowledge, the hVWD1 mice are the first model expressing fully humanized VWF and GPIbα.

Consistent with previous data,[16,17,38] expression of hGPIbα in mice is associated with slightly perturbed platelet count and size but had no functional hemostatic effects (*Online Supplementary Figure S4*).

Accurate analysis of multimer profiles is an essential step for VWF studies; however, it remains technically challenging and protocols vary from one laboratory to another. Because hVWD1 mice express hVWF in murine plasma, no perfect reference is available; therefore, we studied VWF multimers in different conditions. Using standard sample dilutions, we confirmed that multimers of all sizes circulate in hVWD1 murine plasma as in human plasma (Figure 2D). Some mouse strains, including the C57Bl/6J, express a less functional ADAMTS13, which is missing the carboxy-terminal thrombospondin type 1 repeat and CUB domains.[21] To overcome this limitation, we generated the hVWD1 mice in a 129S2 genetic background and visualized similar triplet structures in hVWD1 mice as in human plasma (Figure 2D, lanes 3-4).

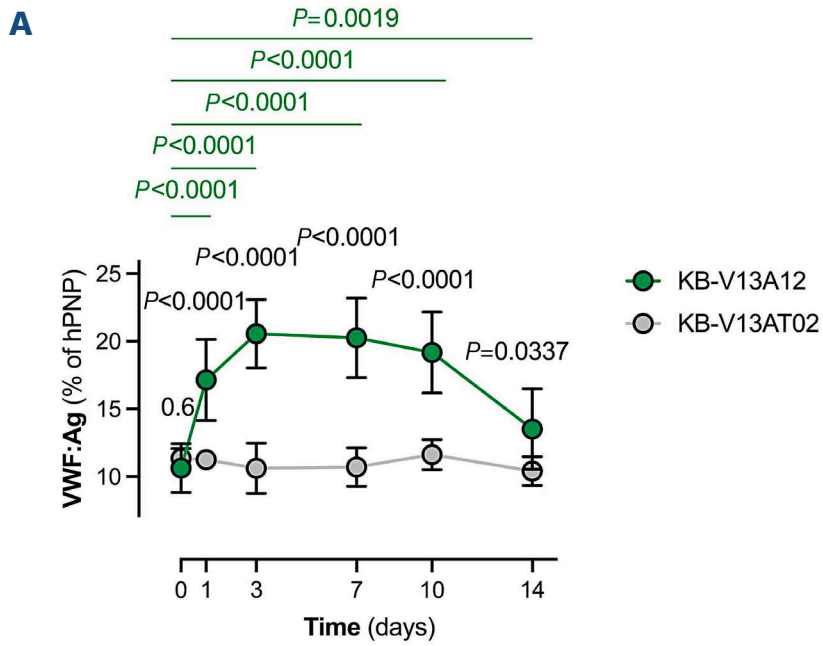

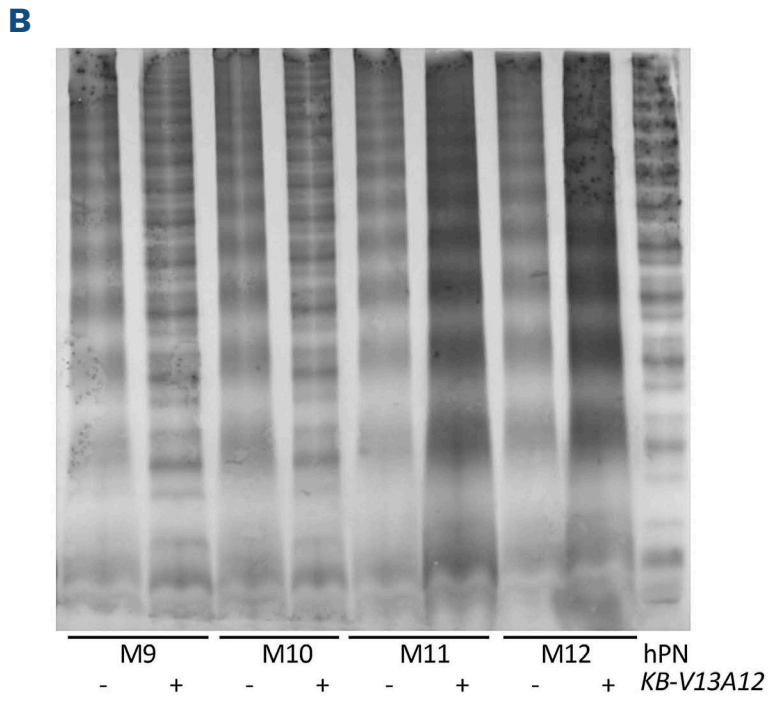

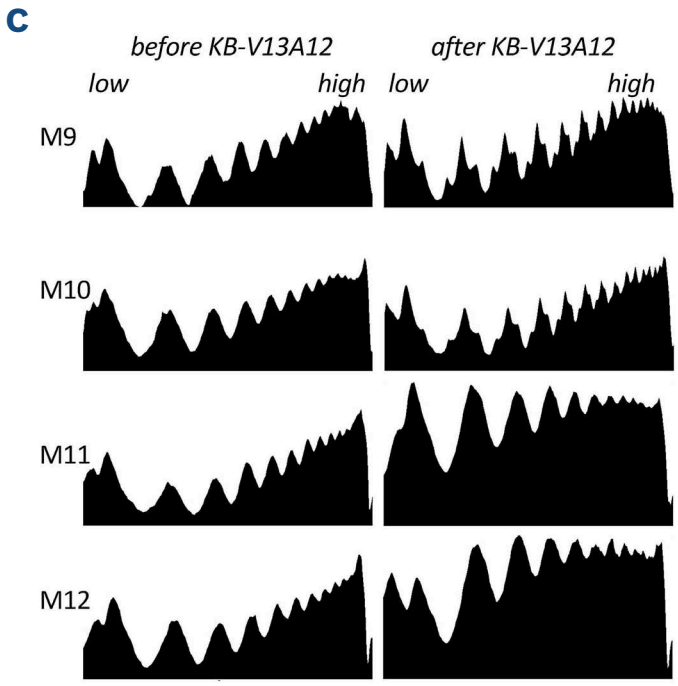

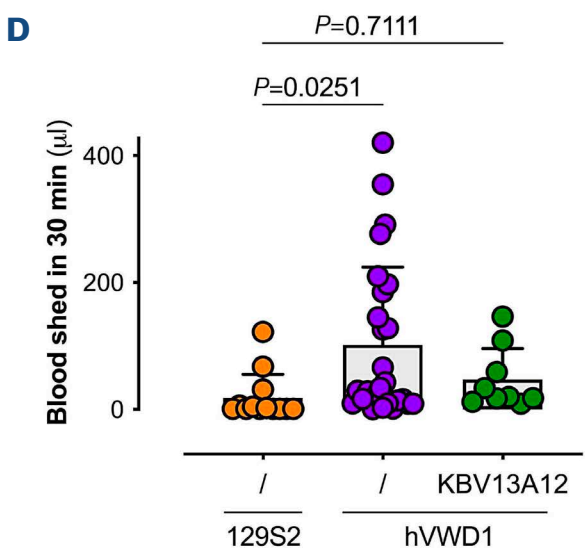

Figure 7. KB-V13A12 modulates von Willebrand factor levels and restores hemostasis in hVWD1 mice. (A) Von Willebrand factor (VWF) antigen levels in von Willebrand disease-type 1 (hVWD1) mice before and post KB-V13A12 (N=15-17, green) or control/KB-V13AT02 (N=3-4, gray) administration at indicated time points. (B) Representative multimer profiles in 2% agarose gel. Colorimetric detection. M9-M10: non-standard sample dilution, approximately 13 ng of VWF. M11-M12: standard sample dilution 10-30 ng of VWF. (C) Densitometric analysis of multimers in (B). Profiles on the left are before and profiles on the right are three days post KB-V13A12 infusion. (D) Amount of blood shed in 30 minutes by control mice (N=13, yellow), untreated hVWD1 mice (N=26, purple) and treated hVWD1 mice (N=9, green). (A) Dots indicate mean±standard deviation (SD). (D) Gray bars indicate mean±SD. (A) Two-way ANOVA. *P* values in green: VWF:Ag levels in KB-V13A12-receiving mice compared to Time (T)0. *P* values in black: VWF:Ag levels in KB-V13A12- *versus* KB-V13AT02-receiving mice at every time point. (D) One-way ANOVA with Dunnett correction for multiple comparisons. low: VWF-low molecular weight multimers (MWM); high: high MWM.

Patients with VWD-type 1 often experience mucocutaneous bleedings such as bruising, epistaxis, oral bleeds, bleeds from minor wounds and menorrhagia.[4] To evaluate the bleeding tendency of the transgenic mice, we assessed hemostasis in assays of different severity (Figure 3). In the TVT model, the hVWD1 mice have a rather normal response, similar to control mice. In three more severe models, however, hVWD1 mice display a mild-to-moderate bleeding tendency, consistent with a large proportion of patients' phenotypes. We also observed that in hVWD1 mice, as in patients, bleeding phenotype is quite variable. This suggests that around 12% VWF:Ag levels likely reflect the threshold amount of VWF necessary to maintain hemostasis in mice, and small variations (7.3-18%, minimum-maximum VWF:Ag range) are sufficient to shift the balance towards bleeding or not. Moreover, other than from plasma, VWF from other physiologic compartments (i.e., endothelial cells and platelets) is present in hVWD1 mice and likely contributes to the hemostatic response. In hVWD1 mice, endothelial-VWF mobilization and contribution was demonstrated by the correction of the bleeding tendency upon histamine administration (Figure 6), a proxy for desmopressin, the first treatment option for VWD-type 1 patients. For those not responding to desmopressin, VWF concentrates are the best option. Similar to patients, therapeutic doses of r-hVWF corrected the bleeding tendency of hVWD1 mice (Figure 5). Abnormal hemostatic behavior in hVWD1 mice was further confirmed by reduced thrombus formation over collagen surfaces in perfusion assays (Figure 2E-G) and by a delayed response to ferric chloride *in vivo* (Figure 4), which are most likely due to the VWF defect[39] rather than hGPIbα expression.[17,40] Altogether, these experiments validate the hVWD1 transgenic mice as models of VWD-type 1.

In search of innovative therapeutic options that could be safe, efficient and long-acting, we developed a bispecific sdAb[41] (KB-V13A12) that simultaneously binds albumin and VWF. We hypothesized that VWF bridged to albumin by the nanobody should follow albumin in the FcRn-mediated recycling pathway within the endothelial cells[42] and that this mechanism would increase circulating VWF levels. *In vivo*, one subcutaneous administration of KB-V13A12 to hVWD1 mice was associated with a sustained 2-fold increase in VWF:Ag levels for up to ten days and an increase in multimers of all molecular weights (Figure 7A-C). Furthermore, KB-V13A12 was as efficient as r-hVWF and histamine in correcting hemostasis (Figure 7D). Based on these data, we believe that KB-V13A12 has the potential to be a new treatment option for VWD, particularly VWD-type 1.

It is important to emphasize that heterogenous bleeding symptoms may manifest in VWD, including gender-specific bleeding in people with the potential to menstruate, who still experience increased depression, anxiety, and low quality-of-life.[43-46] Because of its effects on circulating VWF levels, we believe that KB-V13A12 should be further investigated in the context of various bleeding symptoms. Several murine models for severe VWD subtypes are currently available and these have been crucial for our understanding of the pathophysiology of VWD.[39,47-50] Here, we report the first humanized murine model for the most common mild/moderate forms of VWD. Besides their help in dissecting molecular pathways, humanized models are very useful for translational research, for testing therapeutic, diagnostic molecules that directly bind their target (i.e., antibodies such as the KB-V13A12). Apart from hVWD1 mice, other variants (type 2A, type 2M or type 2N) could also be developed for this purpose.

Some limitations should be considered when using hVWD1 mice. These mice have a 129Sv genetic background, which complexifies and increases the costs of breeding and colony management. Most *in vivo* assays were originally developed in C57Bl/6 mice and should be internally validated for the 129 mice. The hVWD1 mice expressing around 12% of hVWF exhibit a certain degree of variability in the *in vivo* assays. Therefore, the choice of the specific assay and the number of animals is key in every experiment. Because of the humanization of VWF and GPIbα, the best reference/control condition should be carefully considered for each experiment. As for some VWD-type 1 patients, the molecular mechanism explaining the low VWF levels in the hVWD1 mice is still unclear, which can limit some data interpretation and use.

Our study indicates that, despite some limitations, this humanized model is a unique platform for preclinical testing of innovative therapeutic options overcoming the species/species incompatibility between hVWF and mGPIba.

Disclosures

IP, ODC, CVD, PJ and CC are co-inventors on a patent regarding KB-V13A12, patent under licence.

Contributions

IP, MH, GMC, EP, MC, EB and CC performed experiments and analyzed data. CR performed genotyping. SS, ODC, CVD, PJL and CC conceived and supervised the study. CC wrote the first version of the manuscript. All authors contributed to data interpretation and critically reviewed and approved the final version of the study for publication.

Acknowledgments

The authors thank Frédéric Adam for his insightful assistance with the perfusion experiments, Claire Auditeau, Delphine Borgel & Dominique Lasne for performing the VWF activity test, and Rim Hamze for technical assistance. Some figures were created using BioRender.com.

Funding

This study was funded by the French National Research Agency (Agence Nationale de la Recherche) with the Hospi-

tal-University Research in Health program (Recherche Hospitalo-Universitaire) WILL-ASSIST-HEART ANR-17-RHUS-0011 and ANR-21-CE14-0076-01.

Data-sharing statement

Data are available upon reasonable request to the corresponding author.

References

1. Leebeek FWG, Eikenboom JCJ. von Willebrand's disease. N Engl J Med. 2016;375(21):2067-2080.
2. James PD, Connell NT, Ameer B, et al. ASH ISTH NHF WFH 2021 guidelines on the diagnosis of von Willebrand disease. Blood Adv. 2021;5(1):280-300.
3. Sadler JE, Budde U, Eikenboom JC, et al. Update on the pathophysiology and classification of von Willebrand disease: a report of the Subcommittee on von Willebrand Factor. J Thromb Haemost. 2006;4(10):2103-2114.
4. Bowman ML, James PD. Controversies in the diagnosis of type 1 von Willebrand disease. Int J Lab Hematol. 2017;39(Suppl 1):61-68.
5. Sadler JE. Low von Willebrand factor: sometimes a risk factor and sometimes a disease. Hematology Am Soc Hematol Educ Program. 2009;106-112.
6. Cumming A, Grundy P, Keeney S, et al. An investigation of the von Willebrand factor genotype in UK patients diagnosed to have type 1 von Willebrand disease. Thromb Haemost. 2006;96(5):630-641.
7. Goodeve A, Eikenboom J, Castaman G, et al. Phenotype and genotype of a cohort of families historically diagnosed with type 1 von Willebrand disease in the European study, Molecular and Clinical Markers for the Diagnosis and Management of Type 1 von Willebrand Disease (MCMDM-1VWD). Blood. 2007;109(1):112-121.
8. Flood VH, Christopherson PA, Gill JC, et al. Clinical and laboratory variability in a cohort of patients diagnosed with type 1 VWD in the United States. Blood. 2016;127(20):2481-2488.
9. James PD, Notley C, Hegadorn C, et al. The mutational spectrum of type 1 von Willebrand disease: results from a Canadian cohort study. Blood. 2007;109(1):145-154.
10. James P, Leebeek F, Casari C, Lillicrap D. Diagnosis and treatment of von Willebrand disease in 2024 and beyond. Haemophilia. 2024;30(Suppl 3):103-111.
11. Sidonio RF, Lavin M. Diagnostic pitfalls and conundrums in type 1 von Willebrand disease. Hematology Am Soc Hematol Educ Program. 2022;2022(1):618-623.
12. Sadler JE. Von Willebrand disease type 1: a diagnosis in search of a disease. Blood. 2003;101(6):2089-2093.
13. Abou-Ismail MY, James PD, Flood VH, Connell NT. Beyond the guidelines: how we approach challenging scenarios in the diagnosis and management of von Willebrand disease. J Thromb Haemost. 2023;21(2):204-214.
14. Denis CV, Susen S, Lenting PJ. von Willebrand disease: what does the future hold? Blood. 2021;137(17):2299-2306.
15. Ware J, Russell SR, Marchese P, Ruggeri ZM. Expression of human platelet glycoprotein Ib alpha in transgenic mice. J Biol Chem. 1993;268(11):8376-8382.
16. Ware J, Russell S, Ruggeri ZM. Generation and rescue of a murine model of platelet dysfunction: the Bernard-Soulier syndrome. Proc Natl Acad Sci U S A. 2000;97(6):2803-2808.
17. Kanaji S, Orje JN, Kanaji T, et al. Humanized GPIbα-von Willebrand factor interaction in the mouse. Blood Adv. 2018;2(19):2522-2532.
18. Navarrete AM, Casari C, Legendre P, et al. A murine model to characterize the antithrombotic effect of molecules targeting human von Willebrand factor. Blood. 2012;120(13):2723-2732.
19. Chen J, Tan K, Zhou H, Lo H-F, et al. Modifying murine von Willebrand factor A1 domain for in vivo assessment of human platelet therapies. Nat Biotechnol. 2008;26(1):114-119.
20. Banno F, Kaminaka K, Soejima K, Kokame K, Miyata T. Identification of strain-specific variants of mouse Adamts13 gene encoding von Willebrand factor-cleaving protease. J Biol Chem. 2004;279(29):30896-30903.
21. Zhou W, Bouhassira EE, Tsai H-M. An IAP retrotransposon in the mouse ADAMTS13 gene creates ADAMTS13 variant proteins that are less effective in cleaving von Willebrand factor multimers. Blood. 2007;110(3):886-893.
22. Lenting PJ, Westein E, Terraube V, et al. An experimental model to study the in vivo survival of von Willebrand factor. Basic aspects and application to the R1205H mutation. J Biol Chem. 2004;279(13):12102-12109.
23. Pruthi RK, Daniels TM, Heit JA, Chen D, Owen WG, Nichols WL. Plasma von Willebrand factor multimer quantitative analysis by in-gel immunostaining and infrared fluorescent imaging. Thromb Res. 2010;126(6):543-549.
24. Groot E, Fijnheer R, Sebastian SA, de Groot PG, Lenting PJ. The active conformation of von Willebrand factor in patients with thrombotic thrombocytopenic purpura in remission. J Thromb Haemost. 2009;7(6):962-969.
25. Aymé G, Adam F, Legendre P, et al. A novel single-domain antibody against von Willebrand Factor A1 domain resolves leukocyte recruitment and vascular leakage during inflammation-brief report. Arterioscler Thromb Vasc Biol. 2017;37(9):1736-1740.
26. Muczynski V, Casari C, Moreau F, et al. A factor VIII-nanobody fusion protein forming an ultrastable complex with VWF: effect on clearance and antibody formation. Blood. 2018;132(11):1193-1197.
27. Barbon E, Ayme G, Mohamadi A, et al. Single-domain antibodies targeting antithrombin reduce bleeding in hemophilic mice with or without inhibitors. EMBO Mol Med. 2020;12(4):e11298.
28. Johansen PB, Tranholm M, Haaning J, Knudsen T. Development of a tail vein transection bleeding model in fully anaesthetized haemophilia A mice - characterization of two novel FVIII molecules. Haemophilia. 2016;22(4):625-631.
29. Rayes J, Hollestelle MJ, Legendre P, et al. Mutation and ADAMTS13-dependent modulation of disease severity in a mouse model for von Willebrand disease type 2B. Blood. 2010;115(23):4870-4877.
30. Marx I, Lenting PJ, Adler T, Pendu R, Christophe OD, Denis CV. Correction of bleeding symptoms in von Willebrand factor-deficient mice by liver-expressed von Willebrand factor mutants. Arterioscler Thromb Vasc Biol. 2008;28(3):419-424.
31. Zirka G, Robert P, Tilburg J, et al. Impaired adhesion of neutrophils expressing Slc44a2/HNA-3b to VWF protects against NETosis under venous shear rates. Blood. 2021;137(16):2256-2266.
32. Buyue Y, Whinna HC, Sheehan JP. The heparin-binding exosite of factor IXa is a critical regulator of plasma thrombin generation and venous thrombosis. Blood. 2008;112(8):3234-3241.
33. Ruggeri ZM. The role of von Willebrand factor in thrombus formation. Thromb Res. 2007;120(Suppl 1):S5-S9.

34. Pugh N, Simpson AMC, Smethurst PA, de Groot PG, Raynal N, Farndale RW. Synergism between platelet collagen receptors defined using receptor-specific collagen-mimetic peptide substrata in flowing blood. Blood. 2010;115(24):5069-5079.
35. Peyron I, Casari C, Christophe OD, Lenting PJ, Denis CV. KB-V13A12, a novel nanobody-based therapeutic molecular for the treatment of von Willebrand disease. Int Soc Thromb Haemost. 2023; Online abs(OC):8.3.
36. Sweeney JD, Novak EK, Reddington M, Takeuchi KH, Swank RT. The RIIIS/J inbred mouse strain as a model for von Willebrand disease. Blood. 1990;76(11):2258-2265.
37. Mohlke KL, Purkayastha AA, Westrick RJ, et al. Mvwf, a dominant modifier of murine von Willebrand factor, results from altered lineage-specific expression of a glycosyltransferase. Cell. 1999;96(1):111-120.
38. Kanaji T, Russell S, Ware J. Amelioration of the macrothrombocytopenia associated with the murine Bernard-Soulier syndrome. Blood. 2002;100(6):2102-2107.
39. Denis C, Methia N, Frenette PS, et al. A mouse model of severe von Willebrand disease: defects in hemostasis and thrombosis. Proc Natl Acad Sci U S A. 1998;95(16):9524-9529.
40. Guerrero JA, Shafirstein G, Russell S, et al. In vivo relevance for platelet glycoprotein Ibα residue Tyr276 in thrombus formation. J Thromb Haemost. 2008;6(4):684-691.
41. Peyron I, Kizlik-Masson C, Dubois MD, et al. Camelid-derived single-chain antibodies in hemostasis: mechanistic, diagnostic, and therapeutic applications. Res Pract Thromb Haemost. 2020;4(7):1087-1110.
42. Chaudhury C, Mehnaz S, Robinson JM, et al. The major histocompatibility complex-related Fc receptor for IgG (FcRn) binds albumin and prolongs its lifespan. J Exp Med. 2003;197(3):315-322.
43. Lavin M, Aguila S, Dalton N, et al. Significant gynecological bleeding in women with low von Willebrand factor levels. Blood Adv. 2018;2(14):1784-1791.
44. Roberts JC, Kulkarni R, Kouides PA, et al. Depression and anxiety in persons with Von Willebrand disease. Haemophilia. 2023;29(2):545-554.
45. Lenting PJ, Kizlik-Manson C, Casari C. Towards novel treatment options in von Willebrand disease. Haemophilia. 2022;28(S4):5-10.
46. Casari C, Leung J, James PD. New and emerging therapies for women, girls and people with the potential to menstruate with VWD. Blood Adv. 2023;7(24):7501-7505.
47. Adam F, Casari C, Prévost N, et al. A genetically-engineered von Willebrand disease type 2B mouse model displays defects in hemostasis and inflammation. Sci Rep. 2016;6:26306.
48. Shi Q, Fahs SA, Mattson JG, et al. A novel mouse model of type 2N VWD was developed by CRISPR/Cas9 gene editing and recapitulates human type 2N VWD. Blood Adv. 2022;6(9):2778-2790.
49. Kanaji S, Morodomi Y, Weiler H, et al. The impact of aberrant von Willebrand factor-GPIbα interaction on megakaryopoiesis and platelets in humanized type 2B von Willebrand disease model mouse. Haematologica. 2022;107(9):2133-2143.
50. Slobodianuk TL, Kochelek C, Foeckler J, Kalloway S, Weiler H, Flood VH. Defective collagen binding and increased bleeding in a murine model of von Willebrand disease affecting collagen IV binding. J Thromb Haemost. 2019;17(1):63-71.